Author Manuscript
Author Manuscript
Author Manuscript
Author Manuscript

HHS Public Access
Author manuscript
J Med Chem. Author manuscript; available in PMC 2019 May 02.

Published in final edited form as:
J Med Chem. 2018 June 28; 61(12): 5187–5198. doi:10.1021/acs.jmedchem.8b00042.

Discovery of Highly Potent Pinanamine-Based Inhibitors Against Amantadine- and Oseltamivir- resistant Influenza A Viruses

Xin Zhao[†,‖,§,‡,*], **Runfeng Li**[⊥,‡], **Yang Zhou**[#,‡], **Mengjie Xiao**[‡,†,‖], **Chunlong Ma**[§,Δ], **Zhongjin Yang**[†], **Shaogao Zeng**[‖], **Qiuling Du**[⊥], **Chunguang Yang**[⊥], **Haiming Jiang**[⊥], **Yanmei Hu**[§,Δ], **Kefeng Wang**[†], **Chris Ka Pun Mok**[⊥,▽], **Ping Sun**[†], **Jianghong Dong**[‖], **Wei Cui**[‖], **Jun Wang**[§,Δ], **Yaoquan Tu**[#], **Zifeng Yang**[⊥,*], and **Wenhui Hu**[†,‖,*]

[†]State Key Laboratory of Respiratory Disease, Key Laboratory of Molecular Target & Clinical Pharmacology, School of Pharmaceutical Sciences & The Fifth Affiliated Hospital, Guangzhou Medical University, Guangzhou 511436, P.R. China

[‖]Guangzhou Institutes of Biomedicine and Health, Chinese Academy of Sciences, Guangzhou 510530, P.R. China

[⊥]State Key Laboratory of Respiratory Disease, National Clinical Research Center for Respiratory Disease, Guangzhou Institute of Respiratory Health, the First Affiliated Hospital, Guangzhou Medical University, Guangzhou 510120, P.R. China

[§]Department of Pharmacology and Toxicology, College of Pharmacy, The University of Arizona, Tucson, Arizona 85721, United States

[Δ]BIO5 Institute, The University of Arizona, Tucson, Arizona 85721, United States

[#]Division of Theoretical Chemistry and Biology, School of Biotechnology, Royal Institute of Technology (KTH), AlbaNova University Center, Stockholm SE-100 44, Sweden

[▽]HKU-Pasteur Research Pole, School of Public Health, HKU Li Ka Shing Faculty of Medicine, The University of Hong Kong, 5 Sassoon Road, Hong Kong

ABSTRACT

Influenza pandemic is a constant major threat to public health caused by influenza A viruses (IAV). IAVs are sub-categorized by the surface proteins: hemagglutinin (HA) and neuraminidase (NA), in which they are both essential targets for drug discovery. While it is of great concern that NA inhibitor oseltamivir resistant strains are frequently identified from human or avian influenza virus, structural and functional characterization of influenza HA has raised hopes for new antiviral therapies. In this study, we explored a structure-activity relationship (SAR) of pinanamine-based

[*]**Corresponding Author** zhaoxin2017@foxmail.com. [*] jeffyah@163.com. [*] huwenhui@gzhmu.edu.cn.
[‡]These authors contributed equally.
Author Contributions
The manuscript was written through contributions of all authors. All authors have given approval to the final version of the manuscript.

ASSOCIATED CONTENT
Supporting Information.
The Supporting Information is available free of charge on the ACS Publications website
Details regarding inhibitor synthesis, characterization and 1H NMR and 13CNMR spectra of new compounds (PDF)
Molecular formula strings (CSV)

The authors declare no competing financial interest.

Author Manuscript Author Manuscript Author Manuscript Author Manuscript

antivirals and discovered a potent inhibitor **M090** against amantadine-resistant viruses, including the 2009 H1N1 pandemic strains, and oseltamivir- resistant viruses. Mechanism of action studies, particularly hemolysis inhibition, indicated that **M090** targets influenza HA and it occupied a highly conserved pocket of the HA_2 domain and inhibited virus-mediated membrane fusion by "locking" the bending state of HA_2 during the conformational rearrangement process. This work provides new binding sites within the HA protein and indicates that this pocket may be a promising target for broad-spectrum anti-influenza A drug design and development.

SYNOPSIS

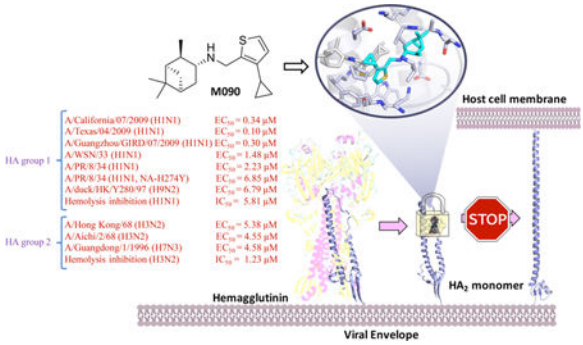

INTRODUCTION

Influenza is a severe respiratory disease caused by influenza viruses. The virus belongs to the *Orthomyxoviridae* family and is an enveloped negative-sense RNA virus.[1] There are three genera of influenza viruses, A, B and C, but only influenza A virus (IAV) causes pandemics.[2] In the last two decades, we have witnessed the outbreak of influenza epidemics and pandemics, such as highly pathogenic avian influenza (HPAI), which occurred in 2005 and 2013 with the subtypes H5N1 and H7N9, respectively.[3,4] Furthermore, in the 2009–2010 influenza season, the H1N1 influenza (swine flu) quickly spread worldwide and caused substantial morbidity and mortality globally.[5] In recent years, another HPAI, H5N6, was identified in the south of China and cases of human infection were reported.[6] Although anti-influenza vaccines are available, the efficacy is limited by antigenic drift or shift of virus.[7,8] Two classes of antiviral drugs are available on the market, the neuraminidase (NA) inhibitors (oseltamivir, zanamivir, and peramivir) and Matrix 2 (M2) ion channel inhibitors (amantadine and rimantadine) (Chart S1). An issue facing both classes of drugs is emerging drug resistance. Nearly all current influenza virus strains are resistant to amantadine and its derivatives.[9–13] The only available orally administered anti-influenza drug, oseltamivir, has been documented to have lost its effect in some strains.[14–16] Therefore, discovery of a novel generation of anti-influenza agents and an understanding of their molecular mechanisms are urgently needed.

Among the list of drug targets that are currently being pursued in preclinical and clinical developments, M2 proton channel remains a hot topic. More than 95% of current circulating influenza A viruses carry the amantadine-resistant AM2-S31N mutation,[17] rendering it a high-profile drug target.[18–28] During the course of developing AM2-S31N inhibitors, it was

Author Manuscript Author Manuscript Author Manuscript Author Manuscript

found that although some of the compounds inhibit viral replication through AM2-S31N channel blockage, there are several analogs that inhibit viral replication through AM2-S31N-independent mechanisms. Following drug resistance testing selection experiments reveal several mutations in hemagglutinin (HA),[29–31] indicating HA might be the drug target instead of M2. Nevertheless, the exact binding site and detailed mechanisms of action of these inhibitors have not yet been fully explored.

Small molecules can be used to probe key features of the mechanism of a specific binding site with a functional protein. Forward chemical genetics operates by using an effective compound to identify the genetic underpinnings of drug targets.[32] Using this approach, in this study, we report our discovery of a potent antiviral, **M090**, and its mechanism of action (MOA). Compound **M090** was discovered through a structure-activity relationship (SAR) study (Table 1) of a series of pinanamine-based antivirals.[33–35] Structural similarity between **M090** and reported AM2-S31N inhibitors led us to hypothesize that **M090** inhibits viral replication through AM2-S31N blockage. However, electrophysiology experiments revealed that **M090** did not inhibit the AM2- S31N channel. Given the potent antiviral activity and the high selectivity index, we therefore are interested in applying **M090** as a chemical probe to dissect its MOA. Through resistance selection experiment, we identified a novel binding pocket that is located at HA_2. The proposed MOA was further supported by molecular dynamics simulations and hemolytic fusion assays. Overall this work suggests a new binding site and the mechanism underlying the interaction of small molecules with the HA protein of IAV and indicates that this more conserved pocket may be an advanced target for antiviral drug design and development.

RESULTS

Chemistry and SAR study.

To study the SAR of pinanamine derivatives using a cytopathic effect (CPE) assay, we conducted a phenotypic screen for synthetic compounds against the swine-origin human influenza A/Guangzhou/GIRD/07/2009 (H1N1)[36] virus. As shown in Scheme 1 and Table 1. The synthesis of pinanamine-heterocyle derivatives (compounds **1** to **10**, Table 1), 5-position substituted thiophene linked derivatives (compounds **35** to **41**, Table 1) and compounds **11, 13, 16, 21, 22, 23, 24, 33** and **34** were obtained from commercially available heterocyclic formaldehyde materials reacting with 3-pinanamine through an easily accessible reductive amination reaction (Method E).[37] For the synthesis of 3- and 4- substituted thiophene derivatives, the routes started from 3-bromothiophene to 3-alkyl substituted thiophene through a Kumada-Corriu coupling reactions (for compounds **19, 20, 31** and **32**, Method A),[38] subsequently, a Vilsmeier–Haack reaction was conducted to afford corresponding 3- (Method B) or 4- (Method C) substituted thiophenecarboxaldehyde (for compounds **12, 14, 15, 25, 26** and **27**),[39] or 3- and 4- substituted thiophenecarboxaldehyde reacted with potassium alkyltrifluoroborate directly (for compounds **17, 18, 28, 29** and **30**, Method D) through a Suzuki-Miyaura cross-coupling reactions (Method A),[40,41] then the same reductive amination reaction gave to the desired compounds (details were described in the Experimental Section).

Author Manuscript Author Manuscript Author Manuscript Author Manuscript

Firstly, we explored the SAR of pinanamine-heterocyle derivatives (compounds **1** to **10**) and identified compound **7** as the most potent compound in primary CPE assay. These results indicated that thiophene group may be a prior pharmacophore. We then further obtained several active compounds through the SAR studies of thiophene based pinanamine derivatives. SAR exhibited that aliphatic substitutions with middle size in the 3- or 4-position (R_1 or R_2 in Table 1) of thiophene revealed potent activities (Table 1). The most potent compound with the highest selectivity index, **M090**, was selected for follow-up inhibition studies on multiple strains (including amantadine-resistant and oseltamivir-resistant strains) of IAV using CPE (Table 2) and a plaque reduction assay (PRA) (Figure 1 and S1). Gratifyingly, **M090** showed potent antiviral activities against A/California/07/2009, H1N1 (amantadine-resistant, oseltamivir- sensitive) and A/Texas/04/2009, H1N1 (amantadine-resistant, oseltamivir-resistant) strains,[42] with an PRA EC_{50} of 0.34 ± 0.016 μM and 0.1 ± 0.009 μM respectively, (Figure 1B and 1C). As the structure of **M090** fits the pharmacophore model of AM2-S31N inhibitors,[26–28] we hypothesize that the broad-spectrum antiviral activity of **M090** might result from its inhibition of the AM2-S31N proton channel. Therefore, we tested the channel blockage of AM2-S31N by **M090** series in two-electrode voltage clamp electrophysiological assay (Table S1).[43] Surprisingly, **M090** showed negligible channel blockage, which suggests its antiviral activity is independent of AM2-S31N channel blockage. Given the broad-spectrum antiviral activity of **M090**, we were intrigued to explore its novel MOA.

Mechanism of Action Study.

The replication cycle of the influenza virus begins at absorption to and ends at the production of its progeny viruses; the whole cycle requires approximately 8 to 10 h. There are three steps, relative to virus entry at time 0, in this process: the early stage of attachment and entry (−1 to 2 h), the middle stage of endosomal release, genome replication and viral protein translation (2 to 8 h), and the late stage of virion assemble and release of progeny viruses (8 to 10 h).[45] Defining −1 h as the time point of absorption, an unbiased drug time-of- addition (TOA) experiment[46] was performed.

The whole life cycle of virus was divided into eight treatment intervals of 1 to 2 h each (Figure 2A); **M090** was administered for treatment, and the yield was measured using $TCID_{50}$ (virus infectious dose that can produce pathological change in 50% of cell cultures inoculated.) testing. The intervals of −1 to 2 h and 0 to 2 h post-virus absorption showed inhibition due to the presence of **M090** (Figure 2B). This finding indicates that M090 blocked the early steps of the virus life cycle, as well as the entry stage, which includes attachment, endocytosis and fusion.[47]

The attachment, endocytosis and fusion process is related to two viral proteins of IAV, M2 and HA.[8,48] As **M090** did not inhibit the AM2-S31N proton channel as shown by the TEVC assay results, we hypothesize that the HA protein may be the target of this series of antiviral compounds such as **M090**. HA is encoded by the fourth viral RNA segment, and its precursor, HA_0, undergoes extra- or intracellular cleavage into two subunits, HA_1 and HA_2.[49,50] In the virus entry progress, HA_1 regulates virus attachment to the sialic acid (SA) receptor of the host cell, which appears as hemagglutination.[51,52] As shown in

Author Manuscript Author Manuscript Author Manuscript Author Manuscript

hemagglutination inhibition (HI) assays, **M090** did not inhibit the virus-induced aggregation of chicken erythrocytes (Figure S2), revealing that there was no interaction between **M090** and the HA_1 domain.

Identification of Binding Sites by Drug Resistance Selection Experiments.

To identify the binding site of **M090**, resistance-induction experiments were performed against the A/Guangzhou/GIRD/07/2009 (H1N1) virus in MDCK cells (Table 3). At each passage, serial 2-fold dilutions of **M090** were selected (43 ~ 0.042 μM) and virus that developed 50% CPE was picked for the subsequent passage. At the first two passages, the virus progeny maintained full drug sensitivity. Drug resistance developed from passage 3, and the EC_{50} increased three-fold. Resistance gradually increased in passages 4 to 6 and became significant after passage 6. After passage 7, the virus was fully resistant to **M090**.

We sequenced the M and HA RNA segments of the resistant strain of passage 8 and compared the sequences with those of the parent A/Guangzhou/GIRD/07/2009 virus, which was reported in the Influenza Research Database.[53] Two substitutions were found (changes in basic groups are shown in Figure S3). Both substitutions occurred in the HA protein, one is A15T, which located at the signal peptide of HA[50] and does not exist in the mature virus protein. Logically, this substitution could not emerge from drug pressure. The other site, HA-E418D, known as HA_2- E74D, is located on the top of the a-helix of the HA_2 trimer (Figure 3). This mutant is the sole reasonable active site of **M090**.

Molecular Dynamics (MD) Simulations.

The potential binding sites of **M090** (Figure 4) were characterized using SiteMap,[55] and **M090** was docked into these sites using Glide.[56] The top-ranked binding poses were clustered. The most favorable docking score in each cluster (Figure S4) was chosen and further refined by MD simulations.

The stability of the predicted conformations of the **M090**-HA_2 complex were evaluated by the average root-mean-square deviation (RMSD) value of HA protein and **M090**. As shown in Figure 5, in the HA_2 monomer, a short helix and a long helix are linked by a loop (Figure 5A). The predicted binding pose of **M090** in the binding pocket is located at the interface of the long helix (residues 82 to 93) and loop (residues 57 to 69) (numbering started from the HA_2 segment). **M090** fits well in the pocket. Its pinane scaffold forms hydrophobic interactions with HA_2-Ala65 and HA_2- Val66, the thiophene ring lays in the hydrophobic region formed by HA_2-Ile89, Tyr312, and HA_2-Trp92, the cyclopropyl group forms hydrophobic interactions with HA_2-Phe88 and Pro303, and the hydrogen bond between N-H and Tyr305 enhances the binding of the compound with the protein (Figure 5B).

During low pH-triggered membrane-fusion, the conformation of the HA2 monomer changes from a folding shape to a needle shape, and HA_2 attaches to the host cell membrane (Figure S5)[57]. Around the experimentally observed **M090**-induced mutant site HA_2-E74, Glu74 directly interacts with the adjacent Arg76 residues to form three hydrogen bonds to stabilize the bent conformation of HA_2 (Figure 6A). MD simulations indicated that in the presence of **M090**, site 1, which is close to the binding pocket, has higher H-bond occupation than the

Author Manuscript Author Manuscript Author Manuscript Author Manuscript

other two binding sites (Figure 6B). Stabilized by **M090**, the initial HA_2 bending state is "locked", and the HA_2 monomer is accordingly blocked to from forming a needle-shaped conformation, which helps the protein attach to the host cell. The *in silico* results are consistent with the experimental drug- resistant mutation E74D, which indicates that the Glu74 mutant is a "shorter form", namely, Asp, and the hydrogen bond interaction is weakened and breaks down easily despite drug binding.

Hemolytic Fusion Assays.

MD simulations demonstrated that **M090** inhibits the membranefusion process by blocking the conformational changes of HA_2; thus, the HA-mediated hemolysis inhibitory effect of **M090** was tested for validation.

The optical density (OD_{540}) value was measured after the chicken red blood cells (CRBC) were mixed with the virus together with different concentrations of **M090**. Two different viral strains (H1N1, A/PR/8/34 and H3N2, A/Aichi/2/68, which represent the two HA phylogenetic groups respectively) were used to induce hemolysis. A known hemolysis inhibitor, Arbidol[58], was used as our control. As shown in Figure 7, the hemolysis inhibition was occurred in dose-dependent manner using the two virus strains.

DISCUSSION

Based on the differences in nucleotide sequences, the HA subtypes are divided into two phylogenetic groups, group 1, including H1, H5 and H9, and group 2, including H3 and H7.[59] Many fusion inhibitors were reported in literature, lots of them were HA group 1 specific, such as **BMS-199945**[60], **RO5464466** series,[61,62] **CL-385319** series[63–65] and so on.[66–71] Recently, a potent peptidic inhibitor of HA was identified, it was also group 1 specific.[72] In the case of group 2, THBQ and its analogues[73–75] and a series of azaspiro derivatives[76] were identified to target H3 subtype. Another broad-spectrum antiviral drug, Arbidol, was characterized as a HA_2 inhibitor.[58] The co-crystallization of it with HA was analyzed and revealed that its binding site was similar with THBQ.[77] We aligned the sequences which cover the potential binding pocket of **M090** from two sets of HA subtype strains, set 1 was comprised of five H1, one H5, one H9 strains, and set 2 was comprised of two H3, two H7 strains (Figure S6). It was found that the sequence similarity of the strains from group 1 was more than 90 % while the strains from group 2 has more than 50% similarity. Remarkably, the escape mutation site, E418, is highly conserved among the two sets. Comparing to the antiviral effect of **M090** on different virus strains including H1 and H9 (belong to group 1) as well as, H3 and H7 (belong to group 2) (Table 2), we found that this region is not absolutely group specific and may be used to design advanced inhibitors that target both phylogenetic groups of HAs and potentially explore broad-spectrum antiviral drugs. At the same time of preparing this paper, a series of aniline-based HA inhibitors were published and reported their antiviral activities against H1 and H5 HAs, the MD simulation study demonstrate that the binding site of these inhibitors overlaps with the binding cavity of THBQ,[78] it may also inhibit the group 2 HA viruses. That work partially support our research strategy and demonstrated the rationality of the new binding site we found. These results can serve as a starting point for our work in coming future including the further

Author Manuscript Author Manuscript Author Manuscript Author Manuscript

optimization of **M090** and its co-crystal complex with HA aiming for the analysis of binding site confirmation.

CONCLUSION

Influenza always threatens causes potential new pandemics and annual epidemics; thus, new therapeutics, especially with new targets and mechanisms of action, constitute a crucial strategy to combat these outbreaks. The process of HA growth and the function of HA offers targets for therapeutic intervention.[79] Here, using a forward chemical genetics approach, we identified a potent antiviral agent, **M090**, and its binding site in the HA_2 subunit. Extensive MOA studies of **M090** indicated that small molecules can bind to a highly conserved segment of HA_2, a new binding site located in the space of the long helix and the loop of the HA_2 monomer. In the presence of inhibitor, low pH-induced membrane fusion was blocked via conformational rearrangements that led to inhibition of HA_2.

This work identifies highly potent inhibitors against amantadine- and oseltamivir-resistant influenza A viruses and provides new insights into the specific binding site of small molecules with HA protein and implications regarding structure-based rational drug design. **M090** and its further-modified compounds potentially could be components in combination therapy with approved anti-influenza drugs to overcome highly pathogenic virus strains. Indeed, this study proposed a promising binding site for the design and development of broad-spectrum antiviral drugs, and these small molecules may have a more resistant genetic barrier under drug pressure due to the conservation of the binding site. In addition, HA contributes to the early stage of the viral cycle, and newly designed HA inhibitors based on this binding site can be used for their prophylactic and therapeutic efficacy.

EXPERIMENTAL SECTION

Chemistry.

All commercially available compounds and solvents were reagent grade and were used without further treatment unless otherwise noted. Reactions were monitored by TLC using Qing Dao Hai Yang GF254 silica gel plates (5 × 10 cm); zones were detected visually under ultraviolet irradiation (254 nm) by either spraying with an ethanol solution of ninhydrin or by treatment with iodine gas. Compounds were purified by silica gel column chromatography performed on silica gel (200 to 300 mesh) from Qing Dao Hai Yang and characterized by ^{1}H NMR, ^{13}C NMR and ESI-MS. The NMR spectra were recorded on a Bruker NMR AVANCE 400 (400 MHz) or a Bruker NMR AVANCE 500 (500 MHz), and the NMR reagents $CDCl_3$ and DMSO-d_6 were used as internal standards. Chemical shifts (δ) were recorded in parts per million and coupling constants (J) in hertz (Hz). MS data were measured on an Agilent MSD-1200 ESI- MS system. The purity of compounds was analyzed by HPLC performed on an Agilent Sunfire C18 (150×4.6mm, 3.5μm) column, solvent, H_2O (0.1 % HCOOH), 0.8 mL/min flow rate or 16 min gradient, 10 % to 100 % TFA in H_2O (10 % to 80% KH_2PO_4 in H_2O for compounds **25** and **37**), 1.0 mL/min flow rate, the peak was detected at 254 nm. All compounds submitted for testing in biological assays were confirmed to be >95% purity by HPLC. Detailed regarding inhibitor

Author Manuscript Author Manuscript Author Manuscript Author Manuscript

characterization are provided in the Supporting Information. For use in assays, compounds were prepared as hydrochlorides or phosphates and dissolved in DMSO.

Detailed synthesis procedures.

Method A.: To a solution of Ni(dppp)Cl_2 (1 mol%) in anhydrous ether (20 mL), in the N_2 atmosphere, Cyclopentylmagnesium chloride or Cyclohexylmagnesium chloride (2M in ether, 30 mmol) was added dropwise at 0 °C, then the 3-Bromothiophene (25 mmol) in ether was added dropwise. The resulting solution was refluxed for 15h, then cooled to r. t. and quenched by 2M HCl. The mixture was extracted using ethyl acetate (100 mL×3). The organic layer was washed with brine, dried with Na_2SO_4 and the solvents were removed. The residue was purified by silica gel column chromatography to afford the corresponding alkylthiophene.

Method B.: To a solution of DMF (5 mL), $POCl_3$ (15 mmol) was added, the mixture was stirred for 1 h at r. t. Then the alkylthiophene (10 mmol) in DMF (5 mL) was added dropwise and stirred for 1 h at 100 °C. The solution was then cooled to 0 °C and quenched by saturated $NaHCO_3$ solution. The mixture was extracted by ethyl acetate (3 × 20 mL), the organic layer was washed with brine, dried with Na_2SO_4 and the solvents were removed. The residue was purified by silica gel column chromatography to afford the corresponding aldehyde.

Method C.: To a solution of alkylthiophene (10 mmol) in anhydrous ether (10 mL), n-BuLi (2M in ether, 15 mmol) was added dropwise at 0 °C in the N_2 atmosphere. The mixture was refluxed for 1 h. The solution was then cooled to r. t. and DMF (1 mL) was added. The resulting solution was stirred for 2 hs and quenched by saturated NH_4Cl solution. The mixture was extracted by ethyl acetate (3 × 20 mL), the organic layer was washed with brine, dried with Na_2SO_4 and the solvents were removed. The residue was purified by silica gel column chromatography to afford the corresponding aldehyde.

Method D.: To a solution of 3- or 4- substituted thiophenecarboxaldehyde (35 mmol), K_3PO_4 (105 mmol), Pd(dppf)Cl_2.CH_2Cl_2 (0.7 mmol) and in toluene/H_2O = 3/1 (140 mL), Potassium Alkyltrifluoroborate (42mmol) was added in the N_2 atmosphere. The resulting solution was refluxed for 10 h. Then 50 mL water was added. Subsequently, the mixture was extracted using ethyl acetate (100 mL×3). The organic layer was washed with brine, dried with Na_2SO_4 and the solvents were removed. The residue was purified by silica gel column chromatography to afford the corresponding alkylthiophene.

Method E.: To a solution of (1R,2R,3R,5S)-(–)-isopinocampheylamine (6.5 mmol) in CH_2Cl_2 (20 mL), aldehyde (1.5 equiv., 9.8 mmol) was added. The reaction mixture was stirred at r.t. for 1 h, followed by the addition of sodium triacetoxyborohydride (26 mmol). The reaction was then stirred for 10 h and quenched by the addition of H_2O and extracted with CH_2Cl_2 (3×20 mL). The combined organic layers were washed with brine, dried with Na_2SO_4 and evaporated to dryness. The residue was purified by silica gel column chromatography, treated with saturated HCl/CH_3OH (20 mL), then evaporated to dryness.

Author Manuscript Author Manuscript Author Manuscript Author Manuscript

The insoluble material was washed with diethyl ether (3×20 mL) to afford the secondary amines as the corresponding hydrochloride salts.

Cytopathic Effect (CPE) Assay.

In the CPE assay, MDCK cells were grown to a confluent monolayer in a 96-well culture plate at a concentration of 5×10^4/well for 24 h. The medium was removed, and the cells were rinsed twice. An infectious virus at 100 $TCID_{50}$ (the influenza virus infectious dose that can produce pathological change in 50% of cells during 48 hours inoculated time period) was inoculated into the MDCK cells, which were then incubated for 2 h at 37 °C in 5% CO_2. The virus supernatant was removed, which was followed by the addition of serial two-fold dilutions of antiviral compounds in DMEM containing 1.5 μg/mL trypsin. After being incubated at 34 °C in 5% CO_2 for 48 h, the infected cells displayed 100% CPE under the microscope, and the CPE percentages in the antiviral compound-treated groups were recorded. The EC_{50} values were calculated using a non-linear regression model in GraphPad Prism.

Cytotoxicity Assay.

The cytotoxicity assay was carried out using similar method as the CPE assay. MDCK cells were grown to a monolayer in a 96-well culture plate at a concentration of 5× 104/well. After 24 hours, the medium was removed, and the cells were rinsed with PBS twice. Compounds with two-fold serial dilution of compounds in DMEM were added into the cells. After incubation for 48 hours, the cell survival rate of each well was observed under the microscope and the concentration which led to minimal change for cell morphology was counted as the minimum cytotoxic concentration.

Plaque Reduction Assay.

A monolayer of A549 cells was infected with 0.01 MOI influenza A viruses for 1 h at 37 °C. The inocula were removed, and the cells were washed twice with phosphate-buffered saline (PBS). The cells were overlaid with 1% agar DMEM with amantadine or one of the synthesized compounds in the presence of 2 μg/mL trypsin and 0.3% BSA. Two to three days after infection, the monolayers were fixed and stained with 0.1% crystal violet solution. The viruses used for this assay were A/California/07/2009 (H1N1) and A/Texas/04/2009 (H1N1). To use the virus strains A/WSN/33 (H1N1), A/HK/68 (H3N2) and A/PR/8/34 (H1N1), MDCK cells were used instead of A549 cells.

Time-of-addition approach.

MDCK cells were grown to a confluent monolayer in a 24-well culture plate and washed twice with PBS. 100 $TCID_{50}$ of influenza A virus (A/PR/8/34) at was inoculated into the MDCK cells (0.5 mL per well) and allowed to absorb at 4 °C for 1 h. The wells were then washed with PBS. The plates received medium containing 1.5 μg/mL TPCK- treated trypsin (0.5 mL per well) and were incubated in a CO_2 incubator at 37 °C for 10 h. Compound (10 μM) was added at −3 to −1, −1 to 0, −1 to 2, 0 to 2, 2 to 4, 4 to 6, 6 to 8, 8 to 10 h post-infection. After each treatment period, the monolayer was washed of drug with PBS, and medium containing 1.5 μg/mL TPCK (0.5 mL per well) was added. After 24 h, the plate was

Author Manuscript Author Manuscript Author Manuscript Author Manuscript

frozen and thawed, the supernatant was collected, and $TCID_{50}$ was measured to determine the virus yield.

Two-Electrode Voltage Clamp (TEVC) Assay.[80]

Selected compounds were tested in a TEVC assay using *Xenopus laevis* frog oocytes microinjected with RNA expressing the wild type or S31N mutant of the A/M2 protein. The potency of the inhibitors was expressed as percentage inhibition of A/M2 current, as observed after 2 min of incubation with 100 Mm compounds at pH 5.5. All measurements were repeated two times with different cells.

Hemagglutination inhibition (HI) assay.

Compound from a serial two-fold dilution in PBS was mixed with an equal volume of influenza virus (A/PR/8/34). After a 1-h incubation in a V- bottom 96-well plate, 50 μL of compound-virus preparation was added to an equal volume of 0.5% freshly prepared chicken red blood cells in Alsever's solution. The mixture was incubated for 40 min at room temperature before observing erythrocyte aggregation on the plate.

Serial passage experiments and resistant mutation identification.

MDCK cells were infected with influenza H1N1 virus (A/Guangzhou/GIRD07/2009) at 100 $TCID_{50}$ for 2 h; the inoculum was removed, and cells were incubated with **M090** at the concentrations of two-fold serial dilutions beginning at MCC or in the absence of **M090** for 2 days to evaluate drug pressure-selected mutations *in vitro.* At the endpoint of each passage, the viruses that developed a significant 50% CPE were harvested and subjected to the following passages. The titer sample of harvested virus at the 8th passage was subjected to sequencing. Influenza viral RNA was isolated using a QIAamp viral RNA Mini Kit (Qiagen, Hilden, Germany). The eight segment cDNAs were generated with reverse-transcription polymerase chain reaction (PCR) using specific primers (Table S2). Reverse-transcription PCR products were identified by agarose gel electrophoresis. PCR products were sequenced by BGI, Inc. (Shenzhen, CHN).

Docking and molecular dynamics (MD) simulations.

The crystal structure of swine-origin A (H1N1)-2009 influenza A virus HA (PDB: 3AL4) was obtained from the Protein Data Bank (http://www.rcsb.org/pdb/) and prepared using the Protein Preparation Wizard.[81] The missing sidechains were added, and the protonation states were determined using PROPKA. The structure thus obtained further underwent a restrained energy minimization. The compound was prepared using LigPrep (Schrödinger, LLC), and 30 conformations were generated for docking. The binding sites were characterized using SiteMap,[55] and all conformations were docked into the active site using Glide.[56]

MD simulations were performed using the GROMACS code.[82] The Amber99SB-ildn force field[83] was used for the protein, and the GAFF force field[84] was used for the compound. Each HA/compound complex was solvated in a 15*15*15 nm^3 cubic box with 144538 TIP3P[85] water molecules. To neutralize the system and to prepare a final NaCl concentration of 0.15 M, 304 Na^+ and 296 Cl^- ions were added. The system was energy minimized with the steepest descent algorithm for 1000 steps. Thereafter, 200-ps isothermal-isochoric (NVT,

Author Manuscript Author Manuscript Author Manuscript Author Manuscript

with T=300 K) and 200-ps isothermal-isobaric (NPT, with T=300 K and P=1 atm) MD simulations were performed to equilibrate the system. The harmonic restraint with a force constant of 1000 kJ mol^{-1} nm^{-2} was used during the simulations. The equilibrated system was then subjected a simulation of 150 ns without any restraint. During the equilibration and production runs, the time step was 2 fs, and the LINCS algorithm[86] was applied to constrain the bonds involving hydrogens. The van der Waals and short-range electrostatic interactions cutoff was set to 10 Å, and the particle-mesh Ewald (PME) method[87] was used to treat long-range electrostatics.

Hemolysis inhibition assay.

A 100-μL influenza virus (A/PR/8/34) or (A/Aichi/2/68) sample was incubated with serial two-fold dilution of compounds in PBS for 30 minutes at 37 °C, and an equal volume of chicken red blood cells with citric acid-sodium citrate (pH 5.0) was added. After incubation at 37 °C for 30 minutes, the mixture was centrifuged (400×g, 8 min, 4 °C). Then, 300 μL of the supernatant was transferred to a 96-well plate, and the absorbance was measured at 540 nm with a Thermo Multiskan MK3 Spectrum spectrophotometer. The value of the mock-infected samples served as the background. IC_{50} was expressed as the compound concentration that caused 50% inhibition of hemolysis.

Supplementary Material

Refer to Web version on PubMed Central for supplementary material.

ACKNOWLEDGMENT

We are grateful for the support of this work by National Natural Science Foundation of China (81302648 to X.Z.; 81761128014 to Zifeng Y.), the State Scholarship Fund of China Scholarship Council (201604910441 to X.Z.), the Youth Innovation Promotion Association CAS (2016319 to X.Z.), the Pearl River S&T Nova Program of Guangzhou (201806010115 to X.Z.), the Ministry of Science and Technology of China (2015DFM30010 to Zifeng Y.), Science research project of the Guangdong Province (2016A050503047 to Zifeng Y.), the Science and Technology Development Fund in Macao Special Administrative Region (084/2015/A to Zifeng Y.), Start-up grant from Guangzhou Medical University (to W.H.), the grant of State Key Laboratory of Respiratory Disease (SKLRD2016ZJ0002 to W.H.). Computer time for this work was awarded by a grant from the Swedish Infrastructure Committee (SNIC) for the project “Modeling of protein-ligand binding” (to Y.T.) and the State Scholarship Fund of China Scholarship Council (201600160013 to Y.Z.). CKP. M. thanks support from Health and Medical Research Fund of Hong Kong (Grant no.17160792). J. W. thanks support from the NIH AI119187.

ABBREVIATIONS

IAV	influenza A viruses
HA	hemagglutinin
NA	neuraminidase
HPAI	highly pathogenic avian influenza
MOA	mechanism of action
SAR	structure-activity relationship
CPE	cytopathic effect

Author Manuscript Author Manuscript Author Manuscript Author Manuscript

PRA	plaque reduction assay
TEVC	two-electrode voltage clamp
TOA	time-of-addition
SA	sialic acid
HI	hemagglutination inhibition
MD	molecular dynamics
PME	particle-mesh Ewald
RMSD	root-mean-square deviation
RBC	red blood cells

REFERENCES

(1). Bouvier N; Palese P The biology of influenza viruses. Vaccine, 2008, 26, D49–D53. [PubMed: 19230160]

(2). Salomon R; Webster RG The influenza virus enigma. Cell 2009, 136, 402–410. [PubMed: 19203576]

(3). Munster VJ; Wallensten A; Baas C; Rimmelzwaan GF; Schutten M; Olsen B; Osterhaus AD; Fouchier RA Mallards and highly pathogenic avian influenza ancestral viruses, northern Europe. Emerg. Infect. Dis. 2005, 11, 1545–1551. [PubMed: 16318694]

(4). Mao C; Wu XY; Fu XH; Di MY; Yu YY; Yuan JQ; Yang ZY; Tang JL An internet-based epidemiological investigation of the outbreak of H7N9 avian influenza A in China since early 2013. J. Med. Internet Res. 2014, 16, e221. [PubMed: 25257217]

(5). https://www.cdc.gov/h1n1flu. Aug 11, 2010.

(6). Yang ZF; Mok CK; Peiris JS; Zhong NS Human infection with a novel avian influenza A(H5N6) virus. N. Engl. J. Med. 2015, 373, 487–489.

(7). Krammer F; Palese P Advances in the development of influenza virus vaccines. Nat. Rev. Drug Discov. 2015, 14, 167–182. [PubMed: 25722244]

(8). De Clercq E Antiviral agents active against influenza A viruses. Nat. Rev. Drug Discov. 2006, 5, 1015–1025. [PubMed: 17139286]

(9). Bright RA; Shay DK; Shu B; Cox NJ; Klimov AI Adamantane resistance among influenza A viruses isolated early during the 2005–2006 influenza season in the United States. J. Am Med. Assoc. 2006, 295, 891–894.

(10). Wan XF; Carrel M; Long LP; Alker AP; Emch M Perspective on emergence and re-emergence of amantadine resistant influenza A viruses in domestic animals in China. Infect. Genet. Evol. 2013, 20, 298–303. [PubMed: 24060734]

(11). Bashashati M; Vasfi Marandi M.; Sabouri F Genetic diversity of early (1998) and recent (2010) avian influenza H9N2 virus strains isolated from poultry in Iran. Arch. Virol. 2013, 158, 2089–2100. [PubMed: 23640582]

(12). Govorkova EA; Baranovich T; Seiler P; Armstrong J; Burnham A; Guan Y; Peiris M; Webby RJ; Webster RG Antiviral resistance among highly pathogenic influenza A (H5N1) viruses isolated worldwide in 2002–2012 shows need for continued monitoring. Antiviral Res. 2013, 98, 297–304. [PubMed: 23458714]

(13). Salter A; Ni Laoi B.; Crowley B Emergence and phylogenetic analysis of amantadine- resistant influenza a subtype H3N2 viruses in Dublin, Ireland, over six seasons from 2003/2004 to 2008/2009. Intervirology 2011, 54, 305–315. [PubMed: 21228542]

Author Manuscript Author Manuscript Author Manuscript Author Manuscript

(14). Baz M; Abed Y; Papenburg J; Bouhy X; Hamelin ME; Boivin G Emergence of oseltamivir-resistant pandemic H1N1 virus during prophylaxis. N. Engl. J. Med. 2009, 361, 2296–2297. [PubMed: 19907034]

(15). Marjuki H; Mishin VP; Chesnokov AP; Jones J; De La Cruz. JA; Sleeman K; Tamura D; Nguyen HT; Wu HS; Chang FY; Liu MT; Fry AM; Cox NJ; Villanueva JM; Davis CT; Gubareva LV Characterization of drug-resistant influenza A(H7N9) variants isolated from an oseltamivir-treated patient in Taiwan. J. Infect. Dis. 2015, 211, 249–257. [PubMed: 25124927]

(16). Pizzorno A; Abed Y; Plante PL; Carbonneau J; Baz M; Hamelin ME; Corbeil J; Boivin G Evolution of oseltamivir resistance mutations in influenza A(H1N1) and A(H3N2) viruses during selection in experimentally-infected mice. Antimicrob. Agents Chemother. 2014, 58, 6398–6405. [PubMed: 25114143]

(17). Furuse Y; Suzuki A; Oshitani H Large-scale sequence analysis of M gene of influenza A viruses from different species: mechanisms for emergence and spread of amantadine resistance. Antimicrob. Agents Chemother. 2009, 53, 4457–4463. [PubMed: 19651904]

(18). Wang J; Ma C; Fiorin G; Carnevale V; Wang T Hu F; Lamb RA; Pinto LH; Hong M; Klein ML; DeGrado WF Molecular dynamics simulation directed rational design of inhibitors targeting drug-resistant mutants of influenza A virus M2. J. Am. Chem. Soc. 2011, 133, 12834–12841. [PubMed: 21744829]

(19). Zhao X; Jie Y; Rosenberg MR; Wan J; Zeng S; Cui W; Xiao Y; Li Z; Tu Z; Casarotto MG; Hu W Design and synthesis of pinanamine derivatives as anti-influenza A M2 ion channel inhibitors. Antiviral Res, 2012, 96, 91–99. [PubMed: 22982118]

(20). Rey-Carrizo M; Torres E; Ma C; Barniol-Xicota M; Wang J; Wu Y; Naesens L; DeGrado WF; Lamb RA; Pinto LH; Vázquez S 3-Azatetracyclo [5.2.1.1^{5,8}.0^{1,5}] undecane derivatives: from wild-type inhibitors of the M2 ion channel of influenza A virus to derivatives with potent activity against the V27A mutant. J. Med. Chem. 2013, 56, 9265–9274. [PubMed: 24237039]

(21). Wang J; Ma C; Wang J; Jo H; Canturk B; Fiorin G; Pinto LH; Lamb RA; Klein ML; DeGrado WF Discovery of novel dual inhibitors of the wild-type and the most prevalent drug-resistant mutant, S31N, of the M2 proton channel from influenza A virus. J. Med. Chem. 2013, 56, 2804–2812. [PubMed: 23437766]

(22). Wang J; Wu Y; Ma C; Fiorin G; Wang J; Pinto LH; Lamb RA; Klein ML; DeGrado WF Structure and inhibition of the drug-resistant S31N mutant of the M2 ion channel of influenza A virus. Proc. Natl. Acad. Sci. U. S. A. 2013, 110, 1315–1320. [PubMed: 23302696]

(23). Rey-Carrizo M; Barniol-Xicota M; Ma C; Frigolé-Vivas M; Torres E; Naesens L; Llabrés S; Juárez-Jiménez J; Luque FJ; DeGrado WF; Lamb RA; Pinto LH; Vázquez S Easily accessible polycyclic amines that inhibit the wild-type and amantadine- resistant mutants of the M2 channel of influenza A virus. J. Med. Chem. 2014, 57, 5738–5747. [PubMed: 24941437]

(24). Barniol-Xicota M; Gazzarrini S; Torres E; Hu Y; Wang J; Naesens L; Moroni A; Vázquez S Slow but steady wins the race: dissimilarities among new dual inhibitors of the wild-type and the V27A mutatn M2 channels of influenza A virus. J. Med. Chem. 2017, 60, 3727–3738. [PubMed: 28418242]

(25). Hu Y; Wang Y; Fang L; Ma C, Wang J Design and expeditious synthesis of organosilanes as potent antivirals targeting multidrug-resistant influenza A viruses. Eur. J. Med. Chem. 2017, 135, 70–76. [PubMed: 28433777]

(26). Li F; Hu Y; Wang Y; Ma C; Wang J Expeditious lead optimization of isoxazole- containing influenza A virus M2-S31N inhibitors using the Suzuki-Miyaura cross-coupling reaction. J. Med. Chem. 2017, 60, 1580–1590. [PubMed: 28182419]

(27). Li F; Ma C; Hu Y; Wang Y; Wang J Discovery of potent antivirals against amantadine-resistant influenza A viruses by targeting the M2-S31N proton channel. ACS Infect. Dis. 2016, 2, 726–733. [PubMed: 27657178]

(28). Li F; Ma C; DeGrado WF; Wang J Discovery of highly potent inhibitors targeting the predominant drug-resistant S31N mutant of the influenza A virus M2 proton channel. J. Med. Chem. 2016, 59, 1207–1216. [PubMed: 26771709]

(29). Torres E; Duque MD; Vanderlinden E; Ma C; Pinto LH; Camps P; Froeyen M; Vázquez S; Naesens L Role of the viral hemagglutinin in the anti-influenza virus activity of newly

Author Manuscript Author Manuscript Author Manuscript Author Manuscript

synthesized polycyclic amine compounds. Antiviral Res, 2013, 99, 281–291. [PubMed: 23800838]

(30). Torres E; Leiva R; Gazzarrini S; Rey-Carrizo M; Frigolé-Vivas M; Moroni A; Naesens L; Vázquez S Azapropellanes with anti-influenza A virus activity. ACS Med. Chem. Lett, 2014, 5, 831–836.

(31). Kolocouris A; Tzitzoglaki C; Johnson FB; Zell R; Wright AK; Cross TA; Tietjen I; Fedida D; Busath DD Aminoadamantanes with persistent in vitro efficacy against H1N1 (2009) influenza A. J. Med. Chem, 2014, 57, 4629–4639. [PubMed: 24793875]

(32). Walsh DP; Chang YT Chemical genetics. Chem. Rev. 2006, 106, 2476–2530. [PubMed: 16771457]

(33). Hu W; Zeng S; Li C; Jie Y; Li Z; Chen L Identification of hits as matrix-2 protein inhibitors through the focused screening of a small primary amine library. J. Med. Chem. 2010, 53, 3831–3834. [PubMed: 20394375]

(34). Zhao X; Li C; Zeng S; Hu W Discovery of highly potent agents against influenza A virus. Eur. J. Med. Chem. 2011, 46, 52–57. [PubMed: 21094565]

(35). Dong J; Chen S; Li R; Cui W; Jiang H; Ling Y; Yang Z Hu, W. Imidazole-based pinanamine derivatives: discovery of dual inhibitors of the wild-type and drug-resistant mutant of the influenza A virus. Eur. J. Med. Chem. 2016, 108, 605–615. [PubMed: 26722757]

(36). Yang ZF; Zhao J; Zhu YT; Wang YT; Liu R; Zhao SS; Li RF; Yang CG; Li JQ; Zhong NS The tree shrew provides a useful alternative model for the study of influenza H1N1 virus. Virol. J 2013, 10, 111. [PubMed: 23575279]

(37). Li S; Chiu G; Pulito VL; Liu J; Connolly P, J.; Middleton, S. A. 1- Arylpiperazinyl-4-cyclohexylamine derived isoindole-1,3-diones as potent and selective a- 1a/1d adrenergic receptor ligands. Bioorg. Med. Chem. Lett. 2007, 17, 1646–1650. [PubMed: 17254786]

(38). Hölzer B; Hoffmann RW Kumada-Corriu coupling of Grignard reagents, probed with a chiral Grignard reagent. Chem. Commun. 2003, 0, 732–733.

(39). Hays DS; Detty MR Studies towards alkylthiophene-2-carboxaldehydes. reduction of 3-alkenylthiophenes with triethylsilane/trifluoroacetic acid. regioselectivity in formylation reactions of 3-alkylthiophenes. Heterocycles 1995, 40, 925–937.

(40). Fang GH; Yan ZJ; Deng MZ Palladium-catalyzed cross-coupling of stereospecific potassium cyclopropyl trifluoroborates with aryl bromides. Org. Lett, 2004, 6, 357–360. [PubMed: 14748592]

(41). Molander GA; Brown AR Suzuki-Miyaura cross-coupling reactions of potassium vinyltrifluoroborate with aryl and heteroaryl electrophiles. J. Org. Chem. 2016, 71, 9681–9686.

(42). Ma C; Zhang J; Wang J Pharmacological characterization of the spectrum of antiviral activity and genetic barrier to drug resistance of M2-S31N channel blockers. Mol. Pharmacol. 2016, 90, 188–198. [PubMed: 27385729]

(43). Wang J; Cady SD; Balannik V; Pinto LH; DeGrado WF; Hong M Discovery of spiro-piperidine inhibitors and their modulation of the dynamics of the M2 proton channel from influenza A virus. J. Am. Chem. Soc. 2009, 131, 8066–8076. [PubMed: 19469531]

(44). Zhao X; Zhang ZW; Cui W; Chen S; Zhou Y; Dong J; Jie Y; Wan J; Xu Y; Hu W Identification of camphor derivatives as novel M2 ion channel inhibitors of influenza A virus. Med. Chem. Commun. 2015, 6, 727–731.

(45). Shapiro GI; Gurney TJ; Krug RM Influenza virus gene expression: control mechanisms at early and late times of infection and nuclear-cytoplasmic transport of virus- specific RNAs. J. Virol. 1987, 61, 764–773. [PubMed: 3806797]

(46). Daelemans D; Pauwels R; De Clercq E; Pannecouque C A time-of-drug addition approach to target identification of antiviral compounds. Nat. Protoc, 2011, 6, 925–933. [PubMed: 21637207]

(47). Dimitrov DS Virus entry: molecular mechanisms and biomedical applications. Nature Rev. Microbiol. 2004, 2, 109–122. [PubMed: 15043007]

(48). Du J; Cross TA; Zhou HX Recent progress in structure-based anti-influenza drug design. Drug Discov. Today. 2012, 17, 1111–1120. [PubMed: 22704956]

(49). Yang J; Li M; Shen X; Liu S Influenza A virus entry inhibitors targeting the hemagglutinin. Viruses 2013, 5, 352–373. [PubMed: 23340380]

Author Manuscript Author Manuscript Author Manuscript Author Manuscript

(50). Sriwilaijaroen N; Suzuki Y Molecular basis of the structure and function of H1 hemagglutinin of influenza virus. Proc. Jpn. Acad. Ser. B. 2012, 88, 226–249. [PubMed: 22728439]

(51). Pedersen JC Hemagglutination-inhibition test for avian influenza virus subtype identification and the detection and quantitation of serum antibodies to the avian influenza virus. Methods Mol. Biol. 2008, 436, 53–66. [PubMed: 18370041]

(52). Yu M; Si L; Wang Y; Wu Y; Yu F; Jiao P; Shi Y; Wang H; Xiao S; Fu G; Tian K; Wang Y; Guo Z; Ye X; Zhang L; Zhou D Discovery of pentacyclic triterpenoids as potential entry inhibitors of influenza viruses. J. Med. Chem. 2014, 57, 10058–10071. [PubMed: 25383779]

(53). https://www.fludb.org/brc/fluSegmentDetails.spg?ncbiProteinId=ADD92535&decorator=influenza&context=1527208477058. Apr 16, 2014.

(54). Zhang W; Qi J; Shi Y; Li Q; Gao F; Sun Y; Lu X; Lu Q; Vavricka CJ; Liu D; Yan J; Gao GF Crystal structure of the swine-origin A (H1N1)-2009 influenza A virus hemagglutinin (HA) reveals similar antigenicity to that of the 1918 pandemic virus. Protein Cell 2010, 1, 459–467. [PubMed: 21203961]

(55). Halgren TA Identifying and characterizing binding sites and assessing druggability. J. Chem. Inf. Model. 2009, 49, 377–389. [PubMed: 19434839]

(56). Friesner RA; Murphy RB; Repasky MP; Frye LL; Greenwood JR; Halgren TA; Sanschagrin PC; Mainz DT Extra precision glide: docking and scoring incorporating a model of hydrophobic enclosure for protein-ligand complexes. J. Med. Chem. 2006, 49, 6177–6196. [PubMed: 17034125]

(57). Kalani MR, Moradi A, Moradi M & Tajkhorshid E Characterizing a histidine switch controlling pH-dependent conformational changes of the influenza virus hemagglutinin. Biophys. J. 2013, 105, 993–1003. [PubMed: 23972851]

(58). Leneva IA; Russell RJ; Boriskin YS; Hay AJ Characteristics of Arbidol- resistant mutants of influenza virus: implications for the mechanism of anti-influenza action of Arbidol. Antiviral Res. 2009, 81, 132–140. [PubMed: 19028526]

(59). Tong S; Li Y; Rivailler P; Conrardy C; Castillo DA; Chen LM; Recuenco S; Ellison JA; Davis CT; York IA; Turmelle AS; Moran D; Rogers S; Shi M; Tao Y; Weil MR; Tang K; Rowe LA; Sammons S; Xu X; Frace M; Lindblade KA; Cox NJ; Anderson LJ; Rupprecht CE; Donis RO A distinct lineage of influenza A virus from bats. Proc. Natl. Acad. Sci. U S A, 2012, 109, 4269–4274. [PubMed: 22371588]

(60). Cianci C; Yu K-L; Dischino DD; Harte W; Deshpande M; Luo G; Colonno RJ; Meanwell NA; Krystal MJ pH-Dependent changes in photoaffinity labelling patterns of the H1 influenza virus hemagglutinin by using an inhibitor of viral fusion. Virology 1999, 73, 1785–1794.

(61). Zhu L; Li Y; Li S; Li H; Qiu Z; Lee C; Lu H; Lin X; Zhao R; Chen L; Wu J; Tang G; Yang W Inhibition of influenza A virus (H1N1) fusion by benzenesulfonamide derivatives targeting viral hemagglutinin. PLoS One 2011, 6, e29120.

(62). Tang G; Lin X; Qiu Z; Li W; Zhu L; Wang L; Li S; Li H; Lin W; Yang M; Guo T; Chen L; Lee D; Wu J; Yang W Design and synthesis of benzenesulfonamide derivatives as potent anti-influenza hemagglutinin inhibitors. ACS Med. Chem. Lett. 2011,2, 603–607.

(63). Plotch SJ; O'Hara B; Morin J; Palant O; LaRocque J; Bloom JD; Lang SA Jr.; DiGrandi MJ; Bradley M; Nilakantan R; Gluzman Y Inhibition of influenza A virus replication by compounds interfering with the fusogenic function of the viral hemagglutinin. J. Virology 1999, 73, 140–151. [PubMed: 9847316]

(64). Liu S; Li R; Zhang R; Chan CCS; Xi B; Zhu Z; Yang J; Poon VKM; Zhou J; Münch J; Kirchhoff F; Pleschka S; Haarmann T; Dietrich U; Pan C; Du L; Jiang S; Zheng B CL-385319 inhibits H5N1 avian influenza A virus infection by blocking viral entry. Eur. J. Pharmacol. 2011, 660, 460–467. [PubMed: 21536025]

(65). Li R; Song D; Zhu Z; Xu H; Liu S An induced pocket for the binding of potent fusion inhibitor CL-385319 with H5N1 influenza virus hemagglutinin. PLoS One 2012, 7, e41956.

(66). Luo G; Colonno R; Krystal M Characterization of a hemagglutinin-specific inhibitor of influenza A virus. Virology 1996, 226, 66–76. [PubMed: 8941323]

Author Manuscript Author Manuscript Author Manuscript Author Manuscript

(67). Luo G; Torri A; Harte WE; Danetz S; Cianci C; Tiley L; Say S; Mullaney D; Yu K-L; Ouellet C; Dextraze P; Meanwell N; Colonno R; Kyrstal M Molecular mechanism underlying the action of a novel fusion inhibitor of influenza A virus. J. Virol. 1997, 71, 4062–4070. [PubMed: 9094684]

(68). Deshpande MS; Wei J; Luo G; Cianci C; Danetz S; Torri A; Tiley L; Krystal M; Yu K-L; Huang S; Gao Q; Meanwell NA An approach to the identification of potent inhibitors of influenza virus fusion using parallel synthesis methodology. Bioorg. Med. Chem. Lett. 2001, 11, 2393–2396. [PubMed: 11527739]

(69). White KM; De Jesus P; Chen Z; Abreu P Jr.; Barile E; Mak PA; Anderson P; Nguyen QT; Inoue A; Stertz S; Koenig R; Pellecchia M; Palese P; Kuhen K; García-Sastre A; Chanda SK; Shaw ML Potent anti-influenza compound blocks fusion through stabilization of the prefusion conformation of the hemagglutinin protein. ACS Infect. Dis. 2015, 1, 98–109. [PubMed: 25984567]

(70). Basu A; Antanasijevic A; Wang M; Li B; Mills DM; Ames JA; Nash PJ; Williams JD; Peet NP; Moir DT; Prichard MN; Keith KA; Barnard DL; Caffrey M; Rong L; Bowlin TL New small molecule entry inhibitors targeting hemagglutinin-mediated influenza A virus fusion. J. Virol. 2014, 88, 1447–1460. [PubMed: 24198411]

(71). Basu A; Komazin-Meredith G; McCarthy C; Antanasijevic A; Cardinale SC; Mishra RK; Barnard DL; Caffrey M; Rong L; Bowlin TL Molecular mechanism underlying the action of the influenza A virus fusion inhibitor MBX2546. ACS Infect. Dis. 2017, 3, 330–335. [PubMed: 28301927]

(72). Kadam RU; Juraszek J; Brandenburg B; Buyck C; Schepens WBG; Kesteleyn B; Stoops B; Vreeken RJ; Vermond J Goutier W; Tang C Vogels R; Friesen RHE; Goudsmit J; van Dongen MJP; Wilson IA Potent peptidic fusion inhibitors of influenza virus. Science 2017, 358, 496–502. [PubMed: 28971971]

(73). Bodian D; Yamasaki R; Buswell R; Stearns J; White J; Kuntz I Inhibition of the fusion-inducing conformational change of influenza hemagglutinin by benzoquinones and hydroquinones. Biochemistry 1993, 32, 2967–2978. [PubMed: 8457561]

(74). Russell RJ; Kerry PS; Stevens DJ; Steinhauer DA; Martin SR; Gamblin SJ; Skehel JJ Structure of influenza hemagglutinin in complex with an inhibitor of membrane fusion. Proc. Natl. Acad. Sci. U. S. A. 2008, 105, 17736–17741. [PubMed: 19004788]

(75). Antanasijevic A; Hafeman NJ; Tundup S; Kingsley C; Mishra RK; Rong L; Manicassamy B; Wardrop D; Caffrey M Stabilization and improvement of a promising influenza antiviral: making a PAIN PAINless. ACS Infect. Dis. 2016, 2, 608–615. [PubMed: 27759373]

(76). Vanderlinden E; Goktas F; Cesur Z; Froeyen M; Reed ML; Russell CJ; Cesur N; Naesens L Novel inhibitors of influenza virus fusion: structure-activity relationship and interaction with the viral hemagglutinin. J. Virol. 2010, 84, 4277–4288. [PubMed: 20181685]

(77). Kadam RU; Wilson IA Structural basis of influenza virus fusion inhibition by the antiviral drug Arbidol. Proc. Natl. Acad. Sci. U. S. A. 2017, 114, 206–214. [PubMed: 28003465]

(78). Leiva R; Barniol-Xicota M; Codony S; Ginex T Vanderlinden, E. Montes, M.; Caffrey, M.; Javier Luque, F.; Naesens, L. Vázquez, S. Aniline-based inhibitors of influenza H1N1 virus acting on hemagglutinin-mediated fusion. J. Med. Chem. 2018, 61, 98–118. [PubMed: 29220568]

(79). Li F; Ma C; Wang J Inhibitors targeting the influenza virus hemagglutinin. Curr. Med. Chem. 2015, 22, 1361–1382. [PubMed: 25723505]

(80). Balannik V; Lamb RA; Pinto LH The oligomeric state of the active BM2 ion channel protein of influenza B virus. J. Biol. Chem. 2008, 283, 4895–4904. [PubMed: 18073201]

(81). Sastry GM; Adzhigirey M; Day T; Annabhimoju R; Sherman W Protein and ligand preparation: parameters, protocols, and influence on virtual screening enrichments. J. Comput. Aided. Mol. Des. 2013, 27, 221–234. [PubMed: 23579614]

(82). Abraham MJ; Murtola T; Schulz R; Pall S; Smith JC Hess B Lindahl E Gromacs: high performance molecular simulations through multi-level parallelism from laptops to supercomputers. SoftwareX 2015, 1–2, 19–25.

(83). Wickstrom L; Okur A; Simmerling C Evaluating the performance of the FF99SB force field based on NMR scalar coupling data. Biophys. J. 2009, 97, 853–856. [PubMed: 19651043]

Author Manuscript Author Manuscript Author Manuscript Author Manuscript

(84). Wang J; Wang W; Kollman PA; Case DA Automatic atom type and bond type perception in molecular mechanical calculations. J. Mol. Graph. Model. 2006, 25, 247–260. [PubMed: 16458552]

(85). Price DJ; Brooks CL A modified TIP3P water potential for simulation with Ewald summation. J. Chem. Phys. 2004, 121, 10096–10103. [PubMed: 15549884]

(86). Hess B; Bekker H; Berendsen HJC; Fraaije JGEM LINCS: A linear constraint solver for molecular simulations. J. Comput. Chem. 1997, 18, 1463–1472.

(87). Essmann U; Perera L; Berkowitz ML Darden, T.; Lee, H.; Pedersen, L. G. A smooth particle mesh Ewald method. J. Chem. Phys. 1995, 103, 8577–8593.

Author Manuscript Author Manuscript Author Manuscript Author Manuscript

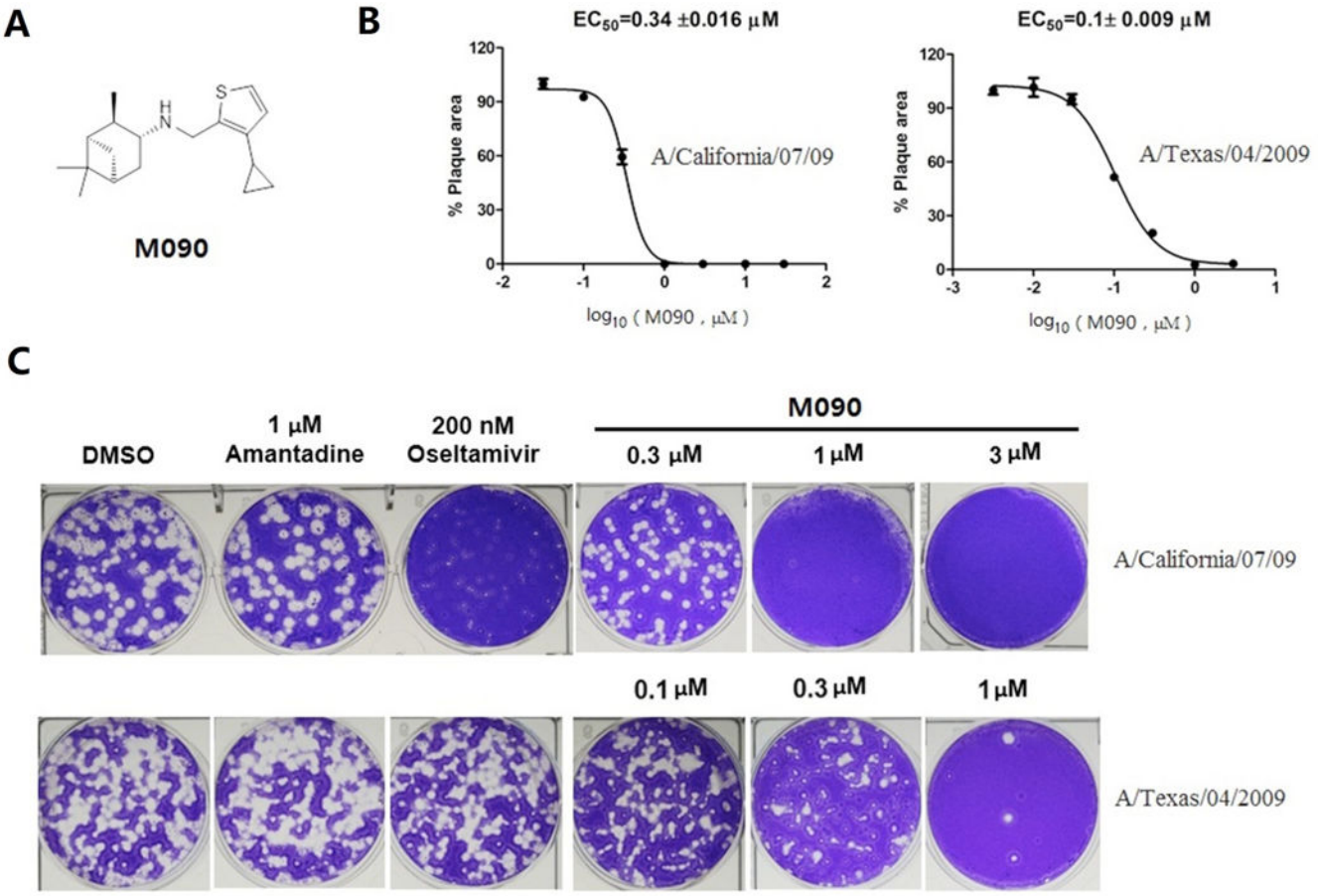

Figure 1.

Identification of **M090** as a potent antiviral against A/California/07/09 and A/Texas/04/2009. (A) Chemical structure of **M090**. (B, C) Inhibitory curves and plaques for **M090**; The EC_{50} was analyzed by measurement of percent area of plaques. Each point corresponds to the mean ± s.d.; data were obtained from two independent experiments.

Author Manuscript Author Manuscript Author Manuscript Author Manuscript

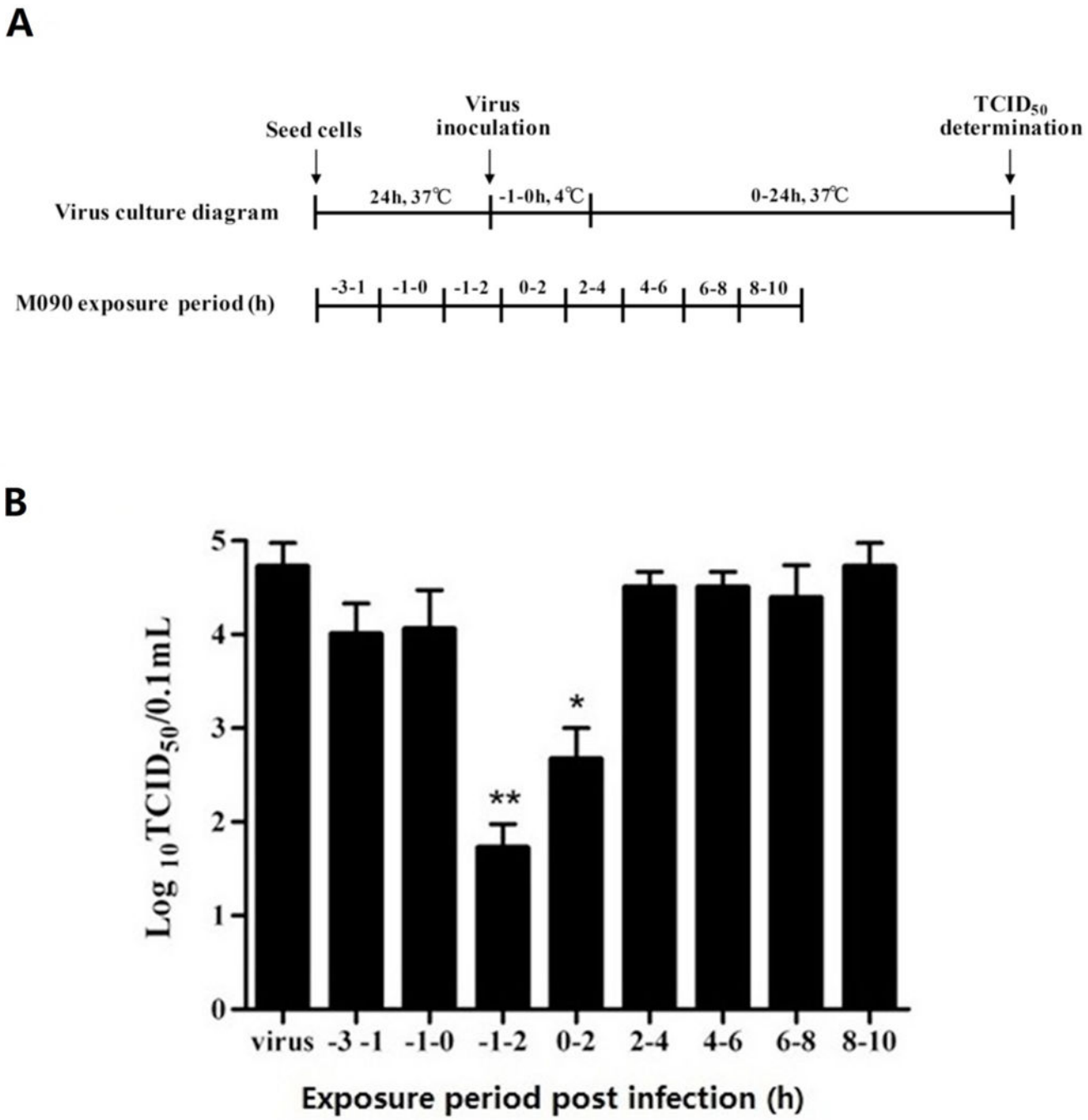

Figure 2. Time-of-addition approach to identify the targeted stage of M090.

(**A**) Time course design. MDCK cells were infected with H1N1 (A/PR/8/34) at 100 $TCID_{50}$. The virus absorption was indicated as −1 h and **M090** was added at −3 to −1, −1 to 0, −1 to 2, 0 to 2, 2 to 4, 4 to 6, 6 to 8, 8 to 10 h post-infection. After each treatment period, **M090** was removed and cells were incubated with culture medium till the end point. (**B**) **M090** was added at each interval, and the virus yield was determined by measuring the $TCID_{50}$. *p<0.05, ** p<0.01, compared to the condition without drug treatment.

Author Manuscript Author Manuscript Author Manuscript Author Manuscript

A

Influenza A virus	Residue substitution in HA induced with M090
A/Guangzhou/GIRD/07/2009	E418D (HA_2-E74D)

B

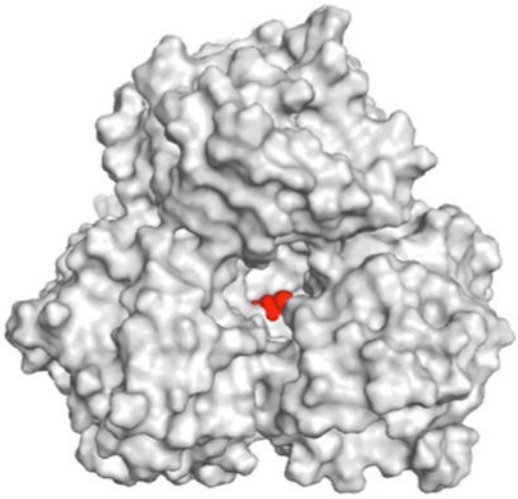

C

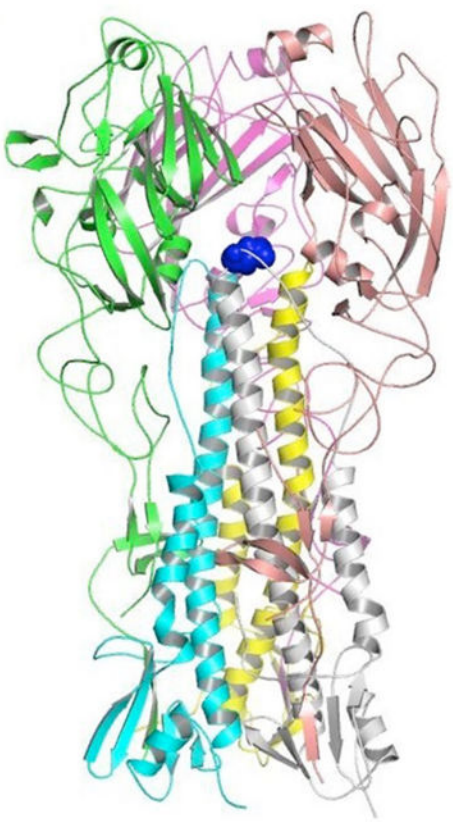

Figure 3. Crystal structure (PDB entry: 3AL4) and M090-induced substitution of HA.

HA structure from the swine-origin A (H1N1)-2009 influenza A virus A/California/04/2009.[54] The RNA sequences of this strain are identical to those of A/California/07/2009 and A/Guangzhou/GIRD/07/2009 that we have used. (**A**) Amino-acid substitution found in HA. (**B, C**) Top and side view of the HA model. The **M090**-resistant site HA_2-E74 is highlighted by spherical models in red and blue, respectively.

Author Manuscript Author Manuscript Author Manuscript Author Manuscript

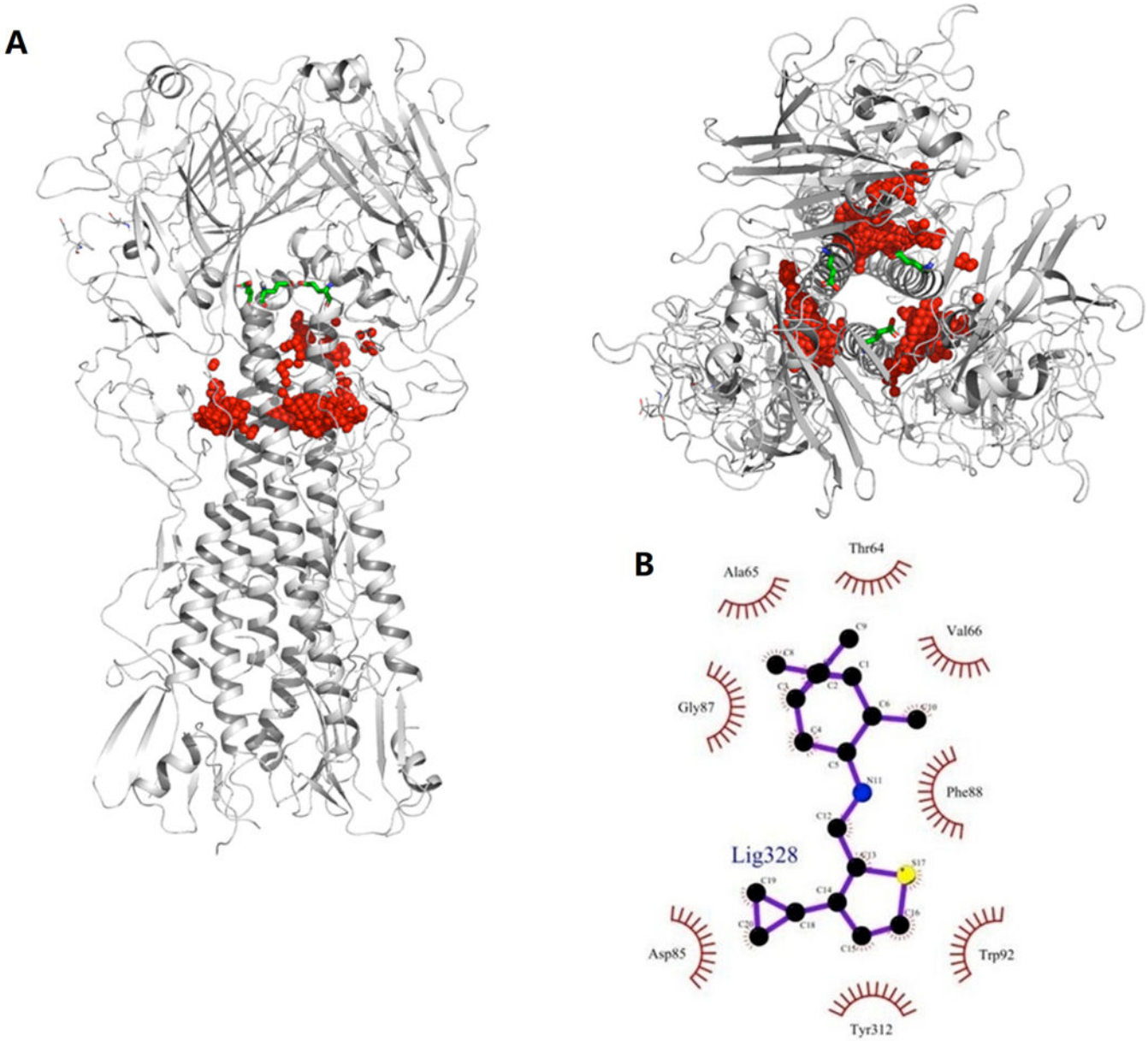

Figure 4. Potential binding sites of M090 in wild type HA protein (PDB entry: 3AL4).

(A) Front and top views of potential binding sites (highlighted in red), HA2-E74 is highlighted by stick model in green. (B) 2D model of the HA binding pocket suggested by docking.

Author Manuscript Author Manuscript Author Manuscript Author Manuscript

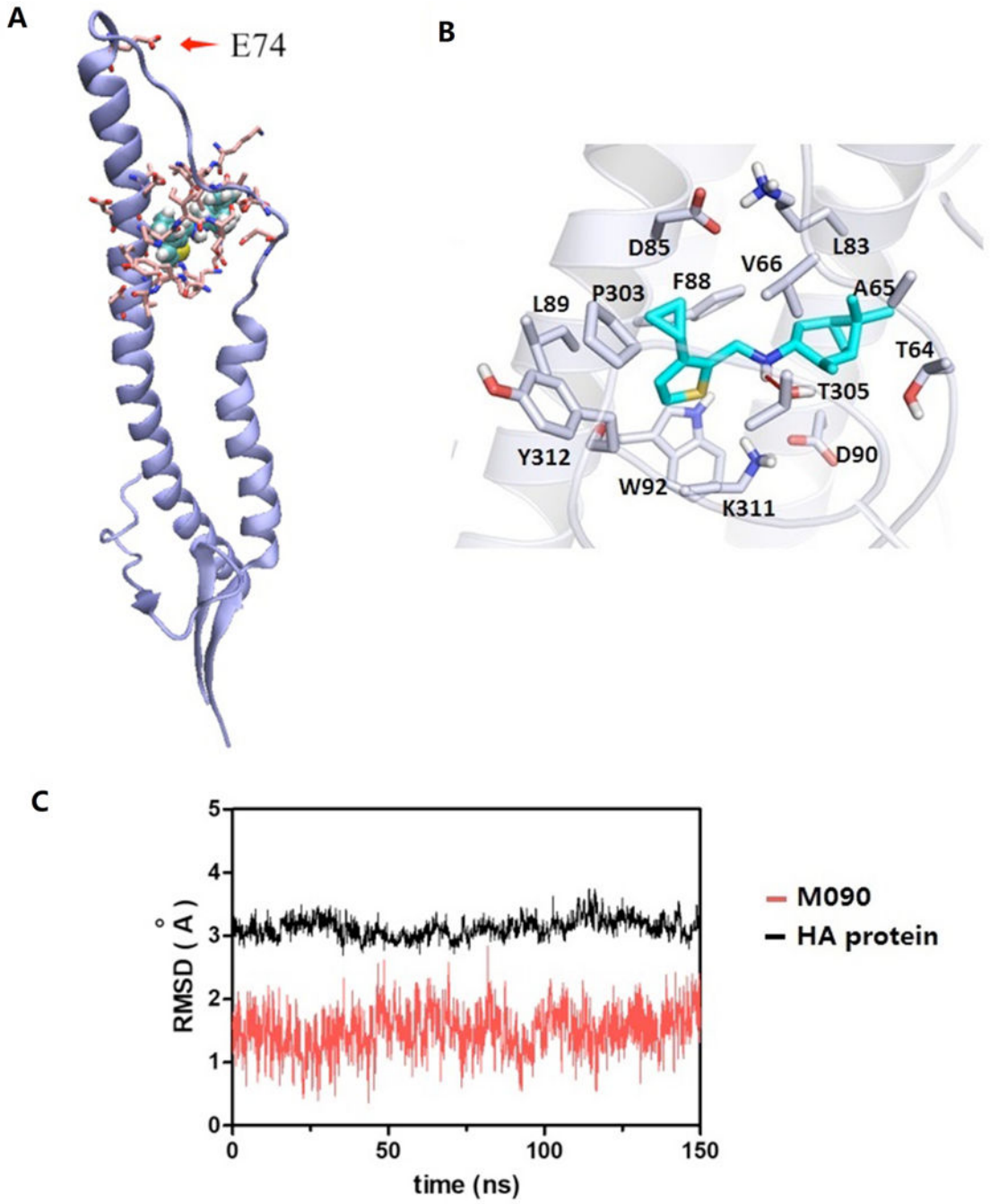

Figure 5. Predicted M090-HA_2 structure.

(A) Adjacent to HA_2-74, **M090** fits well in the pocket between a long α-helical segment and a loop of the HA_2 monomer. (B) Binding mode of **M090** with protein. (C) Time evolution of the RMSD values of **M090** and HA protein during the MD simulation.

Author Manuscript Author Manuscript Author Manuscript Author Manuscript

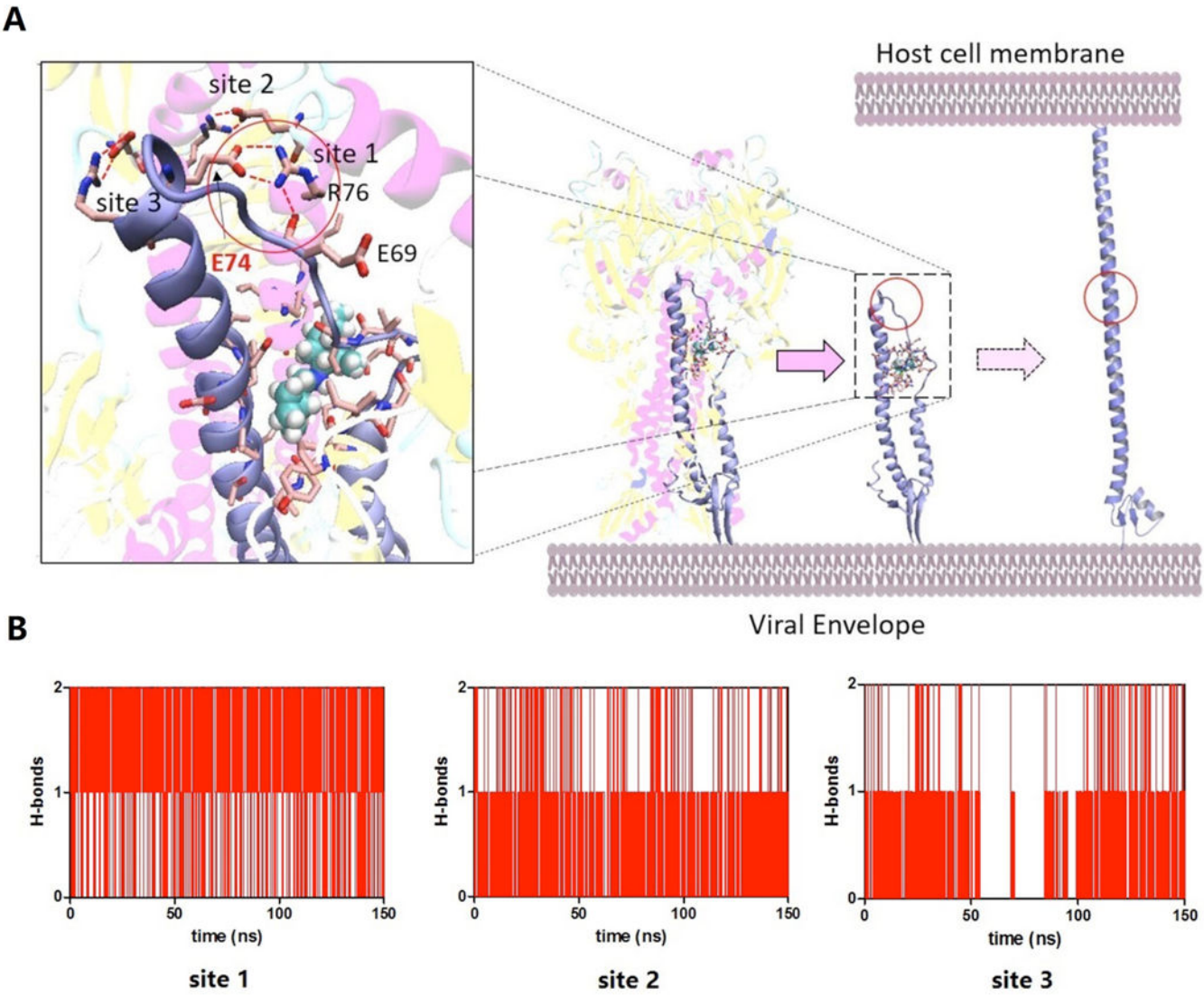

Figure 6. Mode of M090 action studied by MD simulation.

(A) **M090** blocks the conformational change of the HA_2 monomer by enhancing the H-bond interaction between the long helix and the loop. (B) Time evolution of the number of H-bonds of each site during the MD simulation.

Author Manuscript Author Manuscript Author Manuscript Author Manuscript

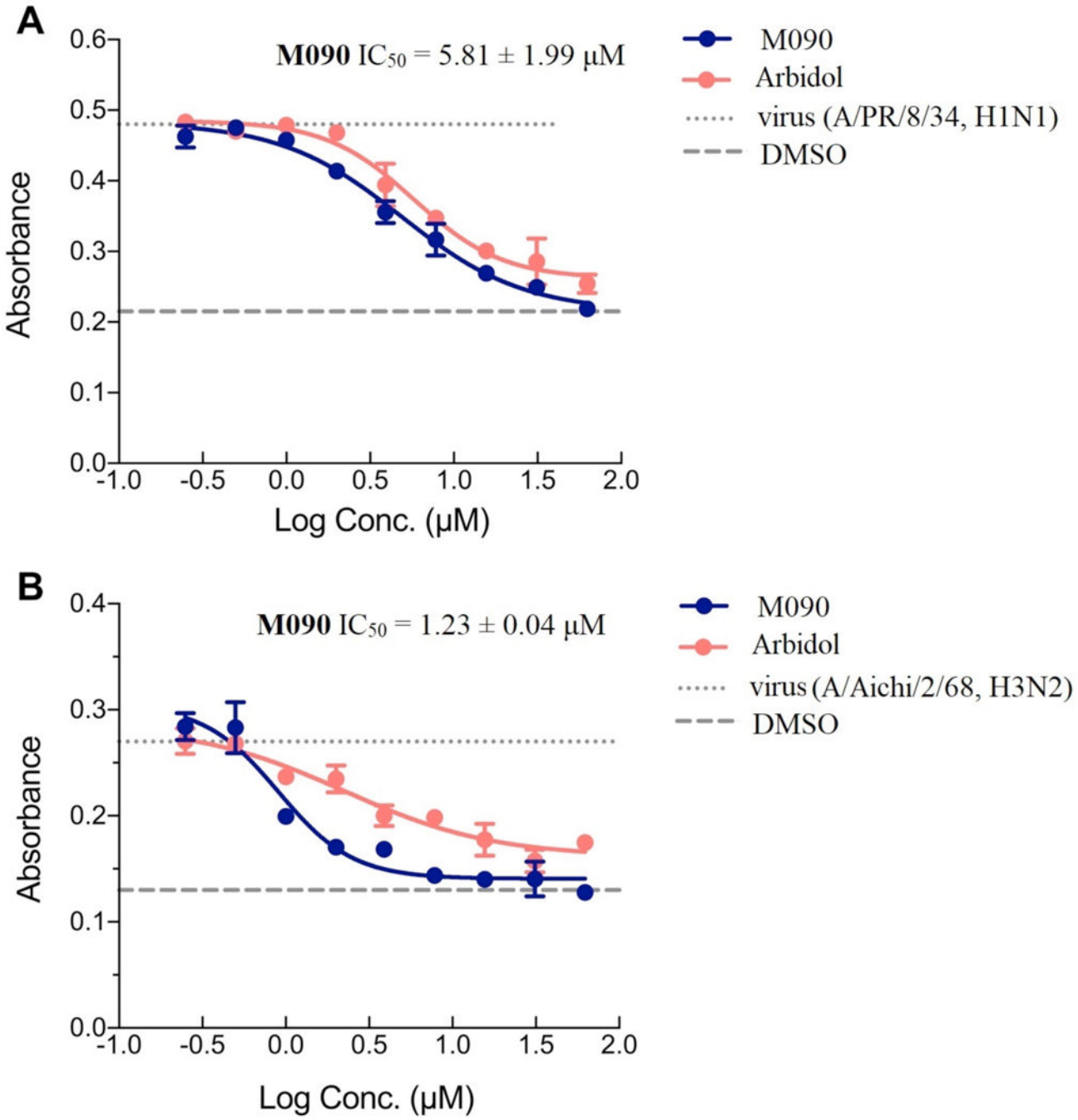

Figure 7. Hemolysis inhibition measurements.

(A) H1N1, A/PR/8/34. (B) H3N2, A/Aichi/2/68. The level of hemolysis inhibition was measured at different concentration of **M090**. At each concentration, the inhibition effect of **M090** (blue curves) was more potent than the positive control, Arbidol (red curves). Each point corresponds to the mean ± s.d.; The results were repeated in two independent experiments.

Author Manuscript Author Manuscript Author Manuscript Author Manuscript

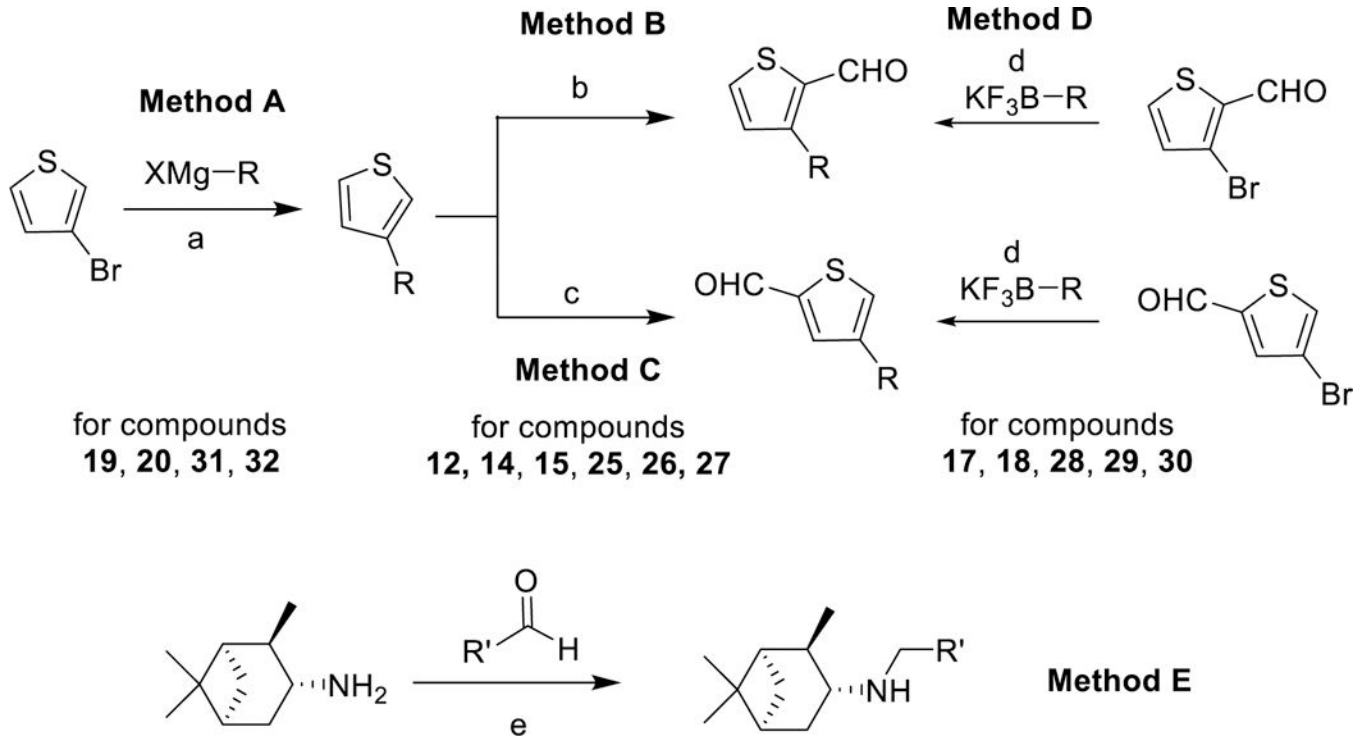

Scheme 1. Synthetic methods of pinanamine derivatives.

Reagents and conditions: (a) $Ni(dppp)Cl_2$, ether, reflux; (b) $POCl_3$, DMF, r.t; (c) *n*-BuLi, −78°C, THF, then DMF; (d) $Pd(dppf)Cl_2$, K_3PO_4, H_2O/toluene=1:3, 100 °C; (e) $NaBH(OAc)_3$, CH_2Cl_2, AcOH, r. t.

Author Manuscript Author Manuscript Author Manuscript Author Manuscript

Table 1.

Inhibitory effect of the synthesized compounds on influenza virus-infected MDCK cells[a].

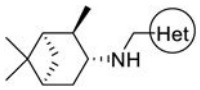

Compd.	Structure	Activity (EC_{50}, μM)[b]	MCC (μM)[c]
1	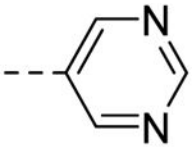	_[d]	>100
2	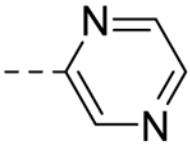	–	>100
3	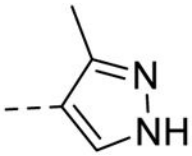	–	>100
4	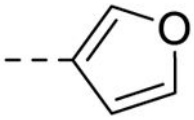	60.46 ± 1.75	>100
5	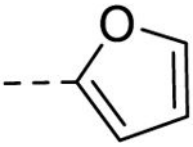	–	50
6	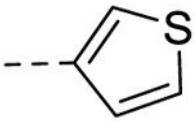	28.60 ±0.24	50

Author Manuscript Author Manuscript Author Manuscript Author Manuscript

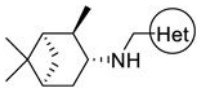

Compd.	Structure	Activity (EC_{50}, μM)[b]	MCC (μM)[c]
7	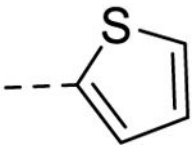	6.42 ± 0.18	25
8	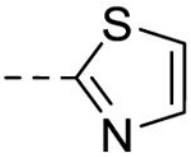	–	>100
9	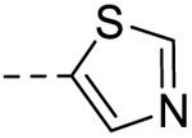	–	>100
10	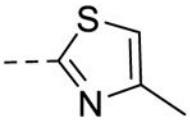	75.00 ± 0.08	>100

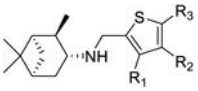

	R_1	R_2	R_3		
11	Me	H	H	–	10
12	Et	H	H	–	25
13	Br	H	H	–	50
14	n-Pr	H	H	–	50
l5	n-Bu	H	H	10.33 ± 2.17	25
16	OEt	H	H	–	50
17	vinyl	H	H	1.82 ± 1.04	50

Author Manuscript Author Manuscript Author Manuscript Author Manuscript

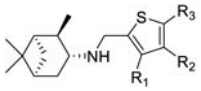

	R_1	R_2	R_3		
18 (M090)	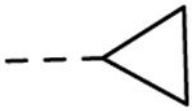	H	H	0.30 ± 0.04	25
19	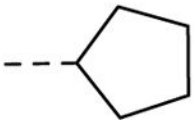	H	H	0.69 ± 0.12	12.5
20	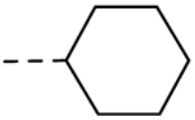	H	H	–	1.56
21	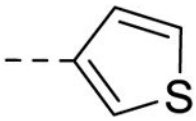	H	H	–	12.5
22	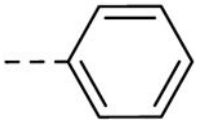	H	H	–	12.5
23	H	Br	H	5.16 ± 1.08	6.25
24	H	Me	H	0.20 ± 0.004	12.5
25	H	Et	H	–	25
26	H	n-Pr	H	–	12.5
27	H	n-Bu	H	0.46 ± 0.07	12.5
28	H	vinyl	H	–	6.25
29	H	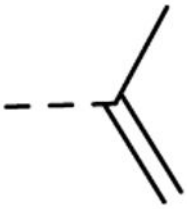	H	–	25

Author Manuscript

Author Manuscript

Author Manuscript

Author Manuscript

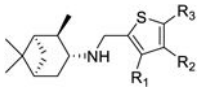

	R_1	R_2	R_3		
30	H	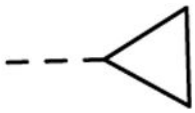	H	6.68 ± 0.42	25
31	H	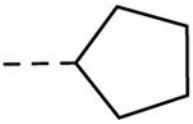	H	–	1.56
32	H	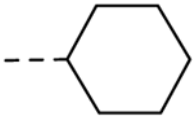	H	–	0.78
33	H	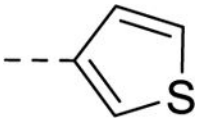	H	–	25
34	H	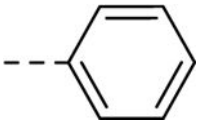	H	–	5
35	H	H	Cl	–	25
36	H	H	Me	–	0.78
37	H	H	Br	–	43
38	H	H	Et	–	1.56
39	H	H	t-Bu	–	0.78
40	H	H	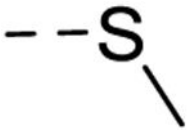	–	25
41	H	H	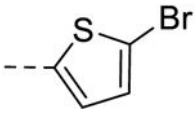	–	0.78

Author Manuscript

Author Manuscript

Author Manuscript

Author Manuscript

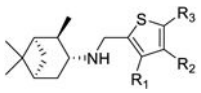

	R_1	R_2	R_3		
Amantadine				>100	>100

[a]Virus strain, A/Guangzhou/GIRD/07/2009 (H1N1).

[b]All the compounds were also tested for the inhibitory effect against A/WSN/33 and A/HK/68 strains based on a CCK-8 reagent measurement method[44]. Compounds **6, 7, 10, 11–18, 23, 24, 26, 28, 30, 36** and **40** exhibited range of micromolar to sub-micromolar activity against both strains (the data were not shown), consistent with this experiment with the Guangzhou strain, compound **18** (**M090**) was the most potent inhibitor of the WSN and HK strains too.

[c]MCC: minimum cytotoxic concentration, or concentration which led to minimal change in cell morphology after 48 h incubation with compound.

[d]"–" represent that no viral inhibition occurs when the concentrations of compounds were lower than MCC.

Author Manuscript

Author Manuscript

Author Manuscript

Author Manuscript

Table 2.

Effect against a broader panel of influenza A viruses.

Compound			M090	Amantadine	Oseltamivir
Antiviral activity (EC_{50}, μM)[a]	H1N1	A/WSN/33	1.48 ± 0.22	>100	0.40 ± 0.08
		A/PR/8/34	2.23 ± 0.60	>100	0.13 ± 0.03
		A/PR/8/34 (NA-H274Y)	6.85 ± 1.85	>100	>10
	H3N2	A/HK/68	5.38 ± 0.32	1.00 ± 0.50	2.30 ± 0.90
		A/Aichi/2/68	4.55 ± 0.80	ND[b]	0.99 ± 0.05
	H7N3	A/duck/Guangdong/1/1996	4.58 ± 0.66	ND	2.67 ± 0.56
	H9N2	A/duck/HK/ Y280/97	6.79 ± 0.44	ND	>10

[a]The anti-influenza activity of **M090** was evaluated by CPE assay and validated by PRA assay (Figure S1).

[b]ND, not detected.

Author Manuscript Author Manuscript Author Manuscript Author Manuscript

Table 3.

Resistance Development under Pressure of M090[a].

Passage no.	EC_{50} (μM)[b]
0	0.30
1	0.34
2	0.32
3	1.70
4	8.70
5	13.8
6	25.6
7	>43.0
8	>43.0
9	>43.0

Resistance to **M090** developed from passage 3 and became significant after passage 6.

[a]The parent strain is A/Guangzhou/GIRD/07/2009.

[b]EC_{50} values tested after each passage.